https://doi.org/10.22364/eeb.23.28

ABSTRACTS
OF THE 6th CONGRESS OF BALTIC MICROBIOLOGISTS

October 1 – 3, 2025, Riga

Effect of enzymatic lactose hydrolysis on microalgal growth in concentrated cheese whey permeate

Sergejs Kolesovs*, Inese Strazdina, Armands Vigants

Institute of Microbiology and Biotechnology, University of Latvia, Jelgavas 1, Riga LV–1004, Latvia
*Corresponding author, E-mail: sergejs.kolesovs@lu.lv

Key words: dairy by-products, *Graesiella emersonii, Galdieria sulphuraria*, lactose, mixotrophic cultivation.

Among various agro-industrial sectors, the dairy industry generates significant amounts of side-streams that remain difficult to valorize. These side-streams require substantial investment in proper treatment, mainly due to their high lactose content, in order to prevent environmental damage upon disposal (Britz et al. 2006).

Microalgal bioconversion can be regarded as a potential solution for the valorization of dairy industry side-streams. Furthermore, this approach may help reduce the production costs of prospective microalgal strains (Kolesovs, Semjonovs 2023). Recent studies have identified that among different microalgal groups, certain strains possess β-galactosidase activity, enabling lactose hydrolysis; however, the number of such strains remains limited, and the biomass productivity is often low. Furthermore, the lack of standardized methodologies for evaluating microalgal growth in dairy side-streams, the absence of standardized media preparation protocols, and the fundamental gaps in understanding microalgal lactose utilization limit the large-scale implementation of this approach (Kolesovs, Semjonovs 2023; Ozcelik et al. 2024).

This study presents a preliminary assessment of enzymatic pretreatment of dairy by-product media, focusing on two lactose-utilizing axenic strains, i.e., the green microalga *Graesiella emersonii* MSCL 1718 and the red microalga *Galdieria sulphuraria* SAG 107.79, with the aim of improving biomass productivity and improving organic carbon (C) removal rates from the media.

Bold's basal medium with triple nitrogen and vitamins (3N-BBM+V) and Allen's Cyanidium medium (ACM) were used as the defined control media for *G. emersonii* and *G. sulphuraria*, respectively (Gross, Schnarrenberger 1995; Kolesovs et al. 2025). Based on previous trials, 3N-BBM+V was supplemented with 30 g L^{-1} lactose, while ACM was supplemented with 20 g L^{-1} lactose. Initially, lactose was dissolved in deionized water and autoclaved for 15 min at 121 °C and 1.2 atm. Subsequently, the 3N-BBM+V and ACM reagent mixtures were added to their respective solutions using a 0.22 µm syringe filter.

Two types of dairy industry by-products, i.e., cheese whey permeate and concentrated permeate, were obtained from a local dairy plant. Our previous evaluations determined the optimal permeate medium preparation strategy for each strain. The concentrated permeate was used for *G. emersonii* due to the microalga's tolerance to high lactose levels, while the non-concentrated permeate was used for *G. sulphuraria* cultivation. The *G. emersonii* medium (P1) was prepared with 20% concentrated cheese whey permeate (*v*/*v*, diluted with deionized water), and supplemented with 0.10 µM $Na_2MoO_4 \times 2H_2O$ (added after sterilization), resulting in lactose concentration of 35g L^{-1}. The P2 medium for *G. sulphuraria* was prepared with 50% cheese whey permeate (*v*/*v*), with lactose concentration of 23 g L^{-1}. The media were sterilized, and lactase enzyme was added under sterile conditions at 0.1 mg mL^{-1} concentration and incubated for 24 h at pH 6.9 ± 0.2. Finally, the enzyme was inactivated by heating the media to 100 °C for 10 min. The pH of P2 was decreased to 4.0 ± 0.1 using 1 M HCl, reaching *G. sulphuraria* optimal pH.

Trials were carried out in 100 mL Erlenmeyer flasks containing 50 mL of media with 10% inoculum (5×10^5 cells mL^{-1}), in an orbital incubator shaker at 25 °C for *G. emersonii* and 42 °C for *G. sulphuraria*, over 12 and 14 days, respectively. Cultures were grown under mixotrophic conditions (12:12 h day-night cycle, 59 ±2 µmol m^{-2} s^{-1} cool white LED light) or heterotrophic conditions. After cultivation, 10 mL biomass samples were collected to determine biomass dry weight (DW, g L^{-1}) and productivity (P, g L^{-1} day^{-1}). Changes in lactose and its monomers were analyzed using enzymatic assay kits for lactose/galactose (K-LACGAR) and glucose (K-GLUC; Megazyme, Ireland). Statistical analyses were performed using IBM SPSS Statistics (Version 29.0.2.0; IBM Corp., Armonk, NY) with one- or two-way ANOVA and Bonferroni post-hoc tests, at a significance level of $p = 0.05$ ($n \geq 4$).

As shown in Fig. 1A, lactose hydrolysis negatively impacted the biomass productivity of *G. emersonii* in the experimental P1 medium (0.28 ± 0.03 g L^{-1} day^{-1})

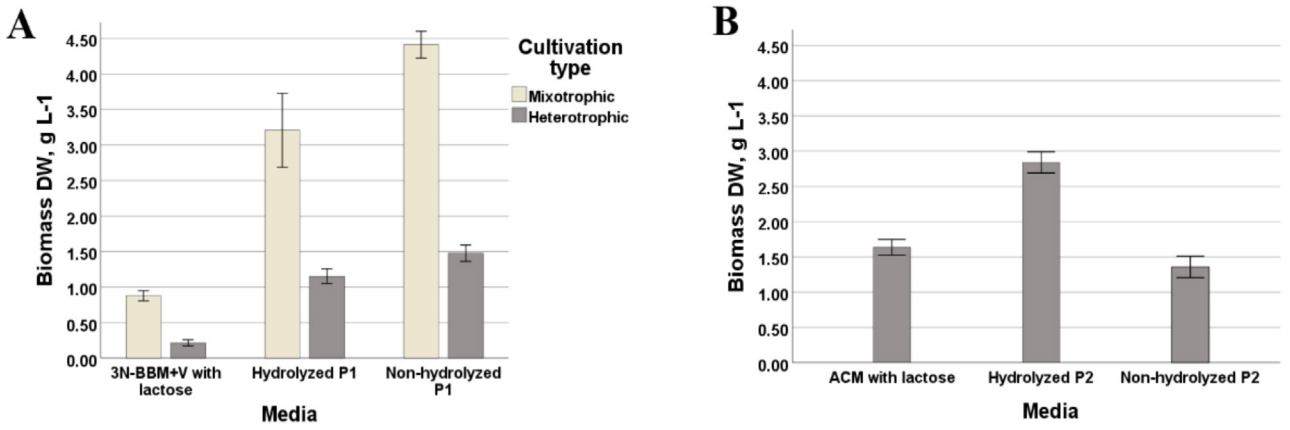

Fig. 1. Comparison of *G. emersonii* biomass synthesis after 12 days of mixotrophic and heterotrophic cultivation in the control 3N-BBM+V medium with lactose and hydrolyzed or non-hydrolyzed P1 media (A). Comparison of *G. sulphuraria* biomass synthesis after 14 days of heterotrophic cultivation in the control ACM medium with lactose and hydrolyzed or non-hydrolyzed P2 media (B).

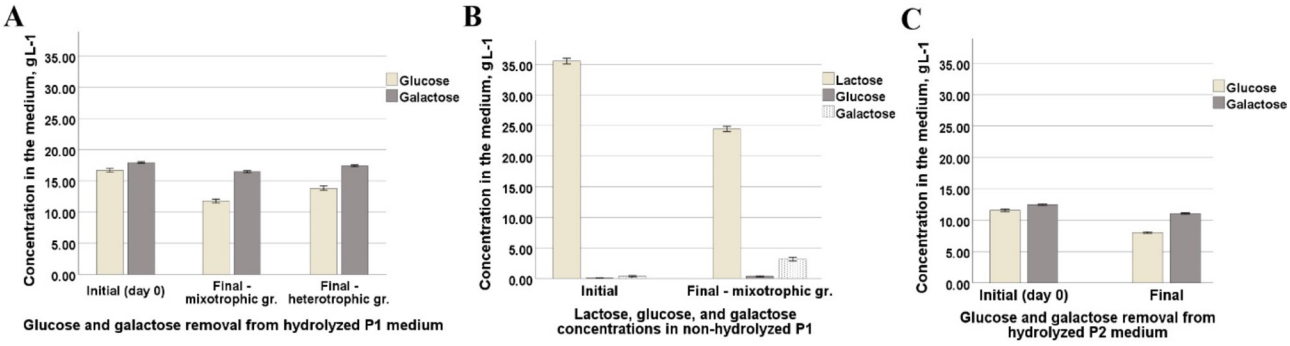

Fig. 2. Changes in monosaccharide (glucose, galactose) concentrations after 12 days of mixotrophic and heterotrophic cultivation of *G. emersonii* in hydrolyzed P1 medium (A). Changes in sugar (lactose, glucose, galactose) concentrations after 12 days of mixotrophic *G. emersonii* non-hydrolyzed P1 medium (B). Changes in monosaccharide (glucose, galactose) concentrations after 14 days of heterotrophic cultivation of *G. sulphuraria* in hydrolyzed P2 media (C).

compared to mixotrophic cultivation in non-hydrolyzed P1 medium (0.35 ± 0.01 g L^{-1} day^{-1}). Overall, the reduction in the biomass productivity was most likely associated with an increase in osmotic pressure; however, higher P1 medium dilutions would deplete other vital nutrients. Therefore, the untreated medium supports more balanced growth and results in significantly higher total C removal under mixotrophic cultivation conditions (Fig. 2A and 2B). On the other hand, lactose hydrolysis has significantly increased *G. sulphuraria* biomass productivity under heterotrophic growth conditions in P2 medium, reaching 0.21 ± 0.01 g L^{-1} day^{-1} and significantly outperforming biomass synthesis in the ACM control medium (Fig. 1B).

Both strains primarily utilized glucose, while galactose remained in the hydrolyzed medium at concentrations close to the initial level (Fig. 2). Furthermore, the accumulation of galactose was detected in the non-hydrolyzed P1 medium (Fig. 2B), which is consistent with our previous findings (Kolesovs et al. 2025), and highlights the fact that galactose utilization is another significant obstacle in dairy by-product bioconversion. Future research will focus on microalgae lacking lactose-metabolizing capabilities, for which enzymatic hydrolysis of lactose-containing media may represent a more impactful cultivation strategy.

References

Britz J.T., van Schalwyk C., Hung Y.T. 2006. Treatment of dairy processing wastewaters. In: Wang L.K., Hung Y.T., Lo H.H., Yapijakis C. (Eds.) *Waste Treatment in the Food Processing Industry*. CRC Press, Boca Raton, FL, USA, pp. 1–25.

Gross W., Schnarrenberger C. 1995. Heterotrophic growth of two strains of the acido-thermophilic red alga *Galdieria sulphuraria*. *Plant Cell Physiol.* 36: 633–638.

Kolesovs, S., Semjonovs, P. 2023. Microalgal conversion of whey and lactose containing substrates: current state and challenges. *Biodegradation* 34: 405–416.

Kolesovs S., Shvirksts K., Grube M., Vigants A. 2025. Studies on lactose utilization by the microalga *Graesiella emersonii* in the 3N-BBM-V model medium. *Eur. J. Phycol.* 60: 175–184.

Ozcelik D., Suwal S., Ray C., Tiwari B.K., Jensen P.E., Poojary M.M. 2024. Valorization of dairy side-streams for the cultivation of microalgae for value added food products. *Trends Food Sci. Technol.* 146: 104386.

Microbial diversity and presence of opportunistic pathogens in ready-to-eat plant-based meat alternatives in Estonia

T. Mandel[1,2], D.N. Sapugahawatte[1], M. Roasto[1]*, M. Mäesaar[1], K. Meremäe[1], T. Elias[1], J. Ruut[1,2], M. Reinik[2]

[1]Chair of Veterinary Biomedicine and Food Hygiene, Institute of Veterinary Medicine and Animal Sciences, Estonian University of Life Sciences, Fr. R. Kreutzwaldi 56/3, 51006 Tartu, Estonia
[2]National Centre for Laboratory Research and Risk Assessment, LABRIS, Fr. R. Kreutzwaldi 30, 51006, Tartu, Estonia
*Corresponding author, E-mail: sergejs.kolesovs@lu.lv

Key words: food safety, microbial diversity, plant -based foods, ready-to-eat, opportunistic pathogens.

The global shift towards plant-based diets has accelerated the development and consumption of plant-derived meat alternatives. These products, designed to mimic traditional meat, have become prominent in modern food markets. Ready-to-eat (RTE) plant-based items, such as cold cuts, burgers, and sausages, are particularly popular due to their convenience and perceived health and environmental benefits (Chen et al. 2025).

Most of these products are classified as ultra-processed foods and undergo intense treatments such as ultra-high-temperature (UHT) or high-pressure processing (HPP) to reduce microbial loads and extend shelf life (Monteiro et al. 2019). However, contamination risk remains during post-processing steps, including slicing, packaging, and storage. Even under controlled conditions, operator or environmental sources can introduce microorganisms that persist in the final product.

Although plant-based RTE foods are generally considered safe, studies show they may harbour microorganisms capable of causing disease in susceptible consumers (Zhao et al. 2025). Most existing research focuses on Western Europe, while information from the Baltic region is limited. This study assessed microbial diversity and the presence of opportunistic bacteria in commercially available RTE plant-based products in Estonia, with special emphasis on meat alternatives, the most common product category in Estonian retail.

Between April 2024 and September 2025, 225 RTE plant-based products (171 meat, 30 dairy, 24 fish alternatives) were purchased from Estonian retail outlets. Product selection covered diverse brands, batches, and formulations. Samples were transported chilled (4 ± 2 °C) to prevent temperature-related microbial growth. For microbiological analysis, 10 g of each product was aseptically homogenised in 90 mL phosphate-buffered saline. Suspensions were serially diluted and plated on selective and non-selective media.

Enumeration and isolation followed ISO protocols targeting aerobic mesophilic bacteria, *Escherichia coli, Bacillus cereus, Clostridium* spp., and *Listeria monocytogenes*. Colonies with distinct morphologies were sub-cultured and identified using MALDI-TOF MS at LABRIS in Tartu. The prevalence of each species was calculated, and organisms were classified according to ecological and clinical relevance.

Despite industrial heat treatment, products displayed diverse microbial profiles. A total of 47 species from 26 genera were identified. The most common isolates included *Bacillus cereus*/*Bacillus thuringiensis* (11.85%), *Leuconostoc mesenteroides* (4.44%), *Staphylococcus hominis* (3.7%), *E. coli* (2.96%), *Proteus vulgaris* (2.22%), *Staphylococcus epidermidis* (2.22%), and *Enterococcus faecium* (1.48%) (Fig. 1).

Most isolates were Gram-positive cocci, consistent with contamination from human contact or processing surfaces. Aerobic mesophilic counts were low (< 10^3 CFU g^{-1}), but ~6% of products exceeded 10^4 CFU g^{-1}, mainly pea-based minced items, which have higher moisture content and bigger surface area.

The findings show that RTE plant-based products harbour microbiota dominated by commensal and opportunistic bacteria. Although species such as *S. hominis, S. epidermidis, E. faecium*, and *Micrococcus luteus* are typical components of human or environmental flora, their presence in processed foods warrants careful interpretation. The frequent detection of coagulase-negative staphylococci suggests post-process contamination, particularly during slicing or packaging, a trend also reported in other RTE food studies (Esemu et al. 2023).

Detection of *E. faecium*, although infrequent, is noteworthy given its opportunistic pathogenicity and

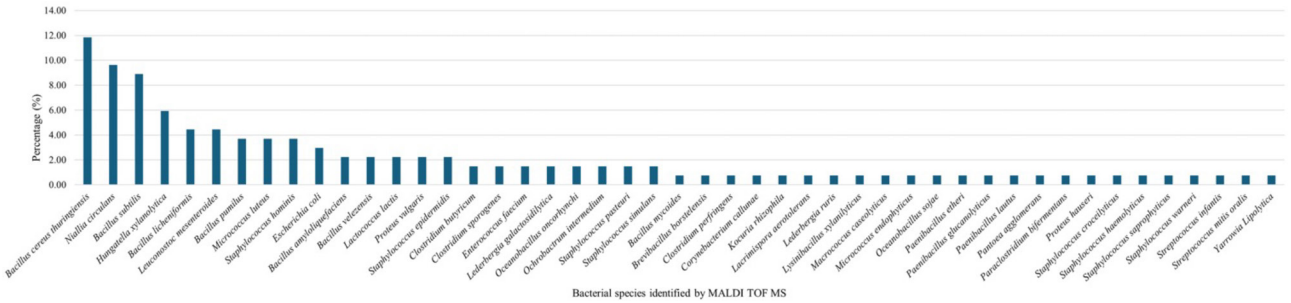

Fig. 1. Relative abundance of bacterial species isolated from RTE plant-based meat alternative samples. The vertical bar chart displays the percentage distribution of each identified bacterial species.

resistance traits. Its presence indicates potential survival through mild processing or environmental contamination. The identification of *Proteus* spp., associated with soil and water, further points to contamination from environmental sources.

Microbial diversity reflected the heterogeneity of producers and raw materials entering the Estonian market. While no *L. monocytogenes* was detected, the presence of *E. coli* (2.96%) and *Clostridium perfringens* (0.74%) shows that processing and preservation steps do not always eliminate major pathogens or spore-formers. Opportunistic species further highlight the importance of environmental hygiene controls.

For healthy consumers, these microorganisms pose limited risk. However, immunocompromised individuals, patients with medical devices, or those on antibiotics may be vulnerable even to low-level contamination. Therefore, assumptions that plant-derived foods are inherently safer than animal-derived products should be avoided.

This study provides the first comprehensive overview of microbial diversity in Estonian RTE plant-based meat alternatives. Although pathogenic bacteria were not detected majorly, a range of opportunistic and commensal species occurred at low concentrations, pointing to post-processing contamination as the most likely source.

Given the rapid growth of the plant-based food sector, routine microbiological monitoring, improved hygiene management, and verification of cleaning and packaging processes are essential. Regular surface and air sampling in production facilities and related corrective actions would reduce recontamination risks. Clear labelling and storage instructions are also necessary to prevent temperature deviations during retail and household storage. Legislative updates may be required to establish specific food safety criteria for alternative products.

Acknowledgements

This work was supported by the EU and Ministry of Education and Research via Project TEM-TA52 „Safety and quality of high-risk plant-based foods and meat alternatives".

References

Chen L., Lin X., Xia Y. 2025. Plant-based meat alternatives: advancements in ingredients, processing, consumer perception, and future directions. *J. Future Foods* 6: 374–388.

Esemu S.N., Njoh S.T., Ndip L. M., Keneh N.K., Kfusi J.A., Njukeng, A. P. 2023. Ready-to-eat foods: a potential vehicle for the spread of coagulase-positive Staphylococci and antimicrobial-resistant *Staphylococcus aureus* in Buea municipality, South West Cameroon. *Canad. J. Infect. Dis. Med. Microbiol.* 2023: 9735319.

Monteiro C.A., Cannon G., Levy R.B., Moubarac J., Louzada M.L., Rauber F., Khandpur N., Cediel G., Neri D., Martinez-Steele E., Baraldi L.G., Jaime P.C. 2019. Ultra-processed foods: what they are and how to identify them. *Public Health Nutr.* 22: 936–941.

Zhao T., Echegaray N., Lorenzo J.M., Köroğlu D.G., Capanoglu E., Ziora Z.M., Esatbeyoglu T. 2025. Exploring meat analogs: a review of alternative proteins with a focus on food safety and regulatory challenges. *Food Contr.* https://doi.org/10.1016/j.foodcont.2025.111777.

Valorisation of low-value plant biomass residues for the development of mycelium-based biocomposites

Ilze Irbe[1]*, Mikus Kampuss[1,2], Inese Filipova[1], Laura Andze[1]

[1]Latvian State Institute of Wood Chemistry, Dzerbenes 27, Riga LV–1006, Latvia
[2]Faculty of Medicine and Life Sciences, University of Latvia, Jelgavas 1, Riga LV–1004, Latvia
*Corresponding author, E-mail: ilze.irbe@kki.lv

Key words: biocomposites, birch sanding dust, mycelium, plant biomass, valorisation, wheat straw.

Mycelium-based biocomposites (MBBs) are natural biomaterials formed through the colonization of wood and non-wood biomass by fungal mycelium. Wood-destroying basidiomycetes are typically used in MBBs fabrication, as they effectively colonize lignocellulosic substrates and generate dense mycelial network (Sydor et al. 2022). This process enables the valorization of low-value agricultural and wood-processing residues into high-value composite materials. Due to their biodegradability, renewability, and low environmental footprint, MBBs represent a sustainable alternative to synthetic polymers in packaging and construction applications (Camilleri et al. 2025).

This study evaluated the physicomechanical properties of MBBs produced from Trametes versicolor mycelium grown on low-value biomass feedstocks: birch sanding dust (BSD) and wheat straw (WS), with co-substrates of hemp shives and birch sawdust. Four different MBB formulations were prepared for each substrate (BSD1 – BSD4 and WS1 – WS4).

Mechanical tests showed that BSD biocomposites exhibited higher compressive (0.10 – 0.24 MPa) (Fig. 1A) and flexural (0.05 – 0.10 MPa) (Fig. 1B) strengths compared to WS composites (0.02 – 0.08 MPa compressive; 0.03 – 0.09 MPa flexural), with the strongest material being BSD1 (0.24 MPa).

The water absorption properties of MBB specimens were determined after 2 h and 24 h immersion (Fig. 2). Absorption within 2 h was a critical duration after which the water uptake of MB was limited. Absorption after 24 h immersion reached up to 600% for BSD2 and 650% for WS2, both with hemp co-substrate.

Hygroscopic sorption analysis showed moisture content between 13 – 17% at 90% relative humidity (RH), rising slightly above 20% at 95% RH, with WS-based composites, particularly WS2, demonstrating higher hygroscopicity to humidity than BSD-based materials (Fig. 3).

In conclusion, mechanical testing demonstrated that BSD biocomposites exhibited higher compressive and flexural strengths compared with WS composites. High water absorption suggested limited use of MBBs in construction without further hydrophobization, but it may be beneficial for applications such as heavy metal

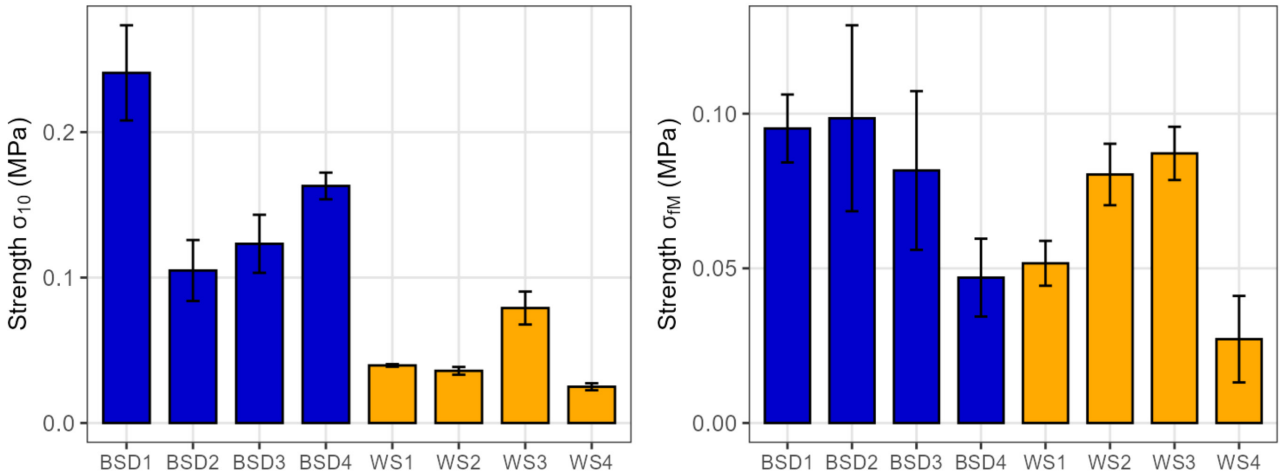

Fig. 1. Compression strength (A) and flexural strength (B) of MBBs. BSD, birch sanding dust; WS, wheat straw; 1 – 4, substrate blends.

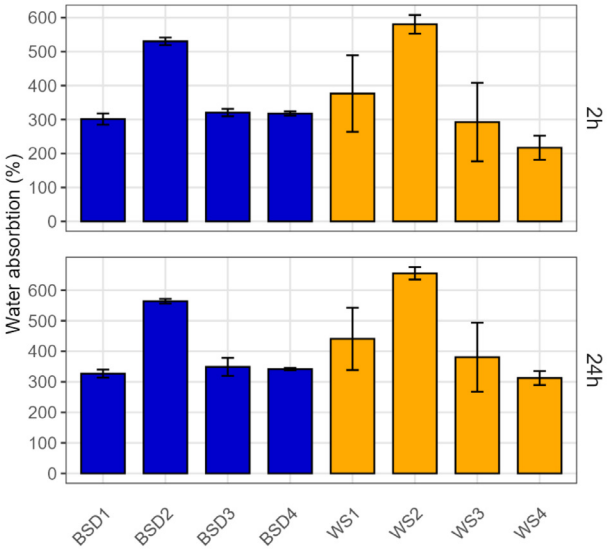

Fig. 2. Water absorption of MBBs. BSD, birch sanding dust; WS, wheat straw; 1 – 4, substrate blends.

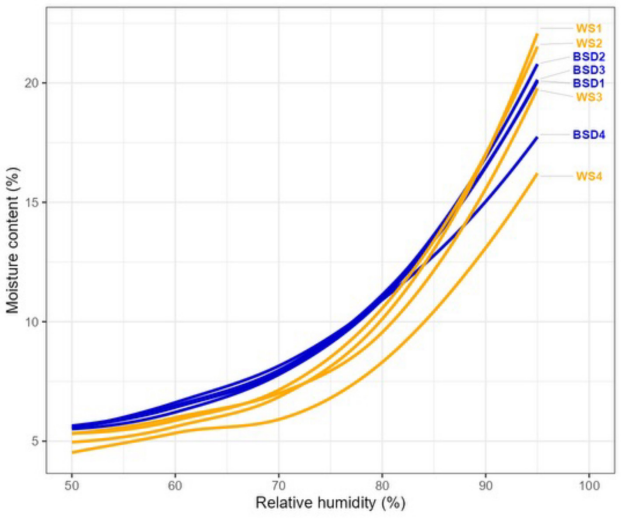

Fig. 3. Adsorption isotherms of MBBs. BSD, birch sanding dust; WS, wheat straw; 1 – 4, substrate blends.

biosorption. The WS-based composites exhibited higher susceptibility to ambient RH compared to the BSD blends. Overall, BSD-based composites provided superior mechanical performance and improved moisture resistance, indicating their greater suitability for biomass residue valorisation in sustainable biocomposite applications.

Acknowledgements

This research was funded by the Latvian Research Council FLPP project No. lzp-2023/1-0633 "Innovative mycelium biocomposites (MB) from plant residual biomass with enhanced properties for sustainable solutions".

References

Sydor M., Cofta G., Doczekalska B., Bonenberg A. 2022. Fungi in mycelium-based composites: usage and recommendations. *Materials* 15: 6283.

Camilleri E., Narayan S., Lingam D., Blundell R. 2025. Mycelium-based composites: an updated comprehensive overview. *Biotechnol. Adv.* 79: 108517.

Effect of substrate composition and chitosan coating on the properties of *Trametes versicolor* mycelium composites

M. Kampuss[1,2]*, A. Verovkins[1], I. Irbe[1]

[1]Cellulose Laboratory, Latvian State Institute of Wood Chemistry, Dzērbenes 27, Riga LV–1006, Latvia
[2]Faculty of Medicine and Life Sciences, University of Latvia, Jelgavas 1, Riga LV–1004, Latvia
*Corresponding author, E-mail: mikusskampuss25@gmail.com

Key words: chitosan coating, mycelium composites, substrate.

Mycelium biocomposites (MBs) are materials composed of fungal mycelium combined with lignocellulosic substrates, in which the fungus functions as a natural adhesive binding the substrate particles. MBs have gained increasing attention as low-cost, environmentally friendly alternatives for use in construction, insulation, packaging, and furniture. Agricultural waste streams serve as suitable, fully biodegradable substrates. Post-processing strongly influences the final properties of MBs; for example, surface coatings can enhance mechanical performance and reduce water absorption (Jones et al. 2020). One promising biodegradable coating is chitosan, a naturally occurring polysaccharide with hydrophobic characteristics (Corazzari et al. 2015).

The aim of this study was to evaluate the effects of substrate type and chitosan coating on the mechanical properties, water absorption behavior, and mycelial abundance within the composites.

Mycelium composites were produced by inoculating sterilized substrates with Trametes versicolor and incubating them under controlled conditions. A detailed description of the process is provided in Irbe et al. (2024). Two substrate types were used: pure wheat straw (WS) and a 1:1 mixture of WS and pine wood chips (commonly used as horse bedding) (WSP), both supplemented with wheat bran. Selected samples were coated with chitosan at varying thicknesses. The thickness of one chitosan layer was approximately 52.83 g m^{-2}. Microscopic analysis of stained and unstained sections was performed using a Leica S9i stereomicroscope (20 ×, 10 MP camera). Lactophenol blue and safranin were used to visualize fungal hyphae and lignin-rich particles, respectively. The staining methods were then compared. ImageJ software was used for image quantification. Mechanical properties (bending and compressive strength) were evaluated using a Zwick/Roell Z010 machine and associated software. Water interactions were assessed through liquid water absorption and hygroscopic response under controlled humidity conditions. Moisture content was calculated based on mass change. Statistical analyses were conducted in RStudio, with differences considered statistically significant at $p < 0.05$.

Lactophenol blue staining provided the highest contrast for quantifying mycelial abundance (Fig. 1), whereas unstained samples were less effective. Safranin staining produced inverse contrast, introducing quantification bias. WS samples exhibited significantly greater mycelial abundance compared to WSP ($p = 0.015$) (Fig. 1).

Water absorption tests showed no strong effect of substrate type, although WSP absorbed slightly more water

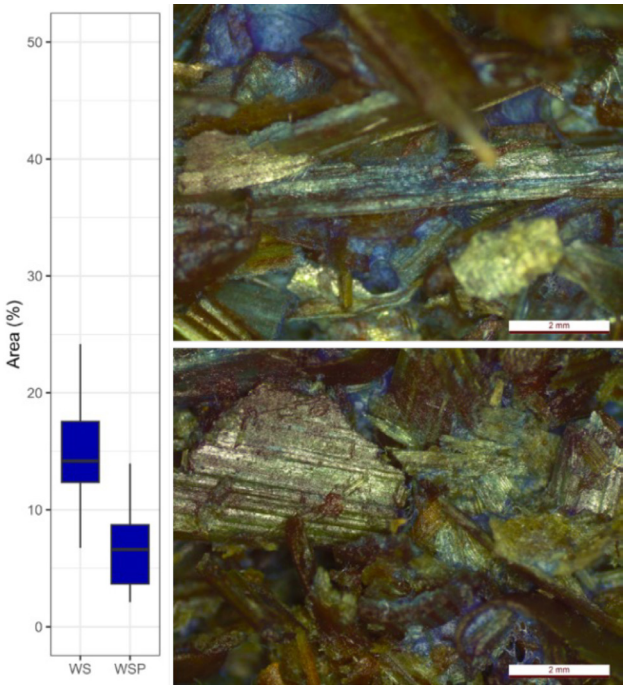

Fig. 1. Microstructure and quantified mycelial abundance in lactophenol-stained WS and WSP samples. WS, wheat straw, WSP, mixture of WS and pine wood chips.

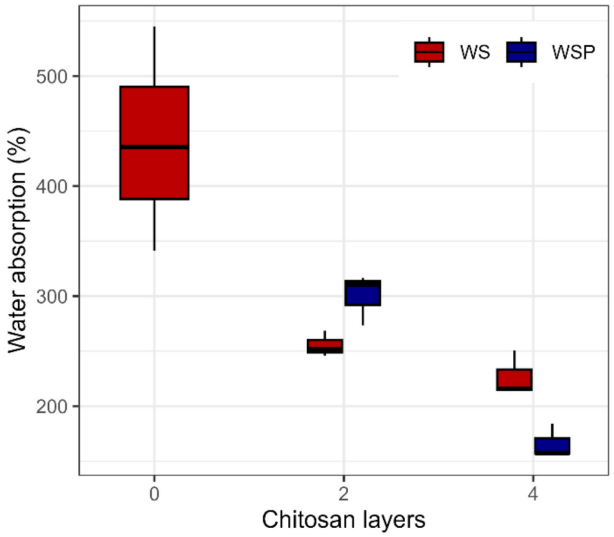

Fig. 2. Water absorption of WS and WSP composites treated with varying amounts of chitosan coating. WS, wheat straw, WSP, mixture of WS and pine wood chips.

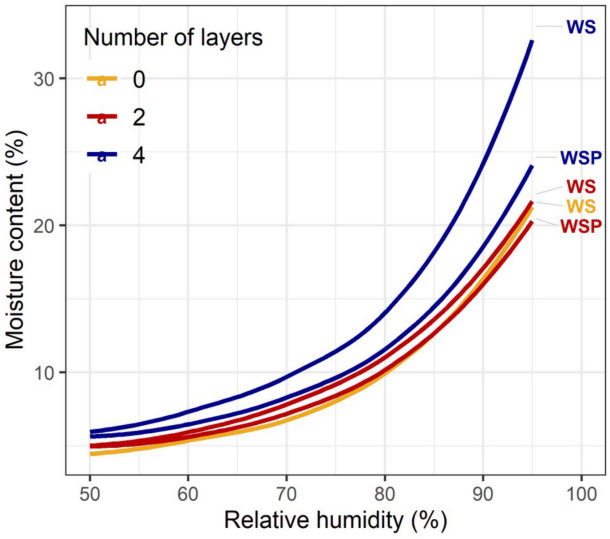

Fig. 3. Moisture uptake from air in WS and WSP composites treated with different amounts of chitosan coating. WS, wheat straw, WSP, mixture of WS and pine wood chips.

(p = 0.053). Chitosan coating significantly reduced liquid water uptake ($p < 0.05$) (Fig. 2). In contrast, hygroscopic analyses revealed that thicker chitosan coatings increased moisture uptake from the air, reaching 36.7% for WS and 25.0% for WSP ($p < 0.05$), thereby exacerbating humidity sensitivity (Fig. 3).

The only significant mechanical difference observed was higher compressive strength in WSP relative to WS.

Acknowledgements

This research was funded by the Latvian Research Council FLPP project No. lzp-2023/1-0633 "Innovative mycelium biocomposites (MB) from plant residual biomass with enhanced properties for sustainable solutions".

References

Corazzari I., Nisticò R., Turci F., Faga M.G., Franzoso F., Tabasso S., Magnacca G. 2015. Advanced physico-chemical characterization of chitosan by means of TGA coupled on-line with FTIR and GCMS: Thermal degradation and water adsorption capacity. *Polymer Degrad. Stabil.* 112: 1-9.

Irbe I., Kirpluks M., Kampuss M., Andze L., Milbreta U., Filipova I. 2024. Assessing the conformity of mycelium biocomposites for ecological insulation solutions. *Materials* 17: 6111.

Jones M., Mautner A., Luenco S., Bismarck A., John S. 2020. Engineered mycelium composite construction materials from fungal biorefineries: A critical review. *Mater. Design* 187: 108397.

Synergistic antimicrobial effect of essential oil blends against skin pathogens

R. Bikmurzin[1,2]*, J. Būdienė[3,4], R. Daunoravičienė[3], I. Pumputienė[1], J. Graželytė[1]

[1]Faculty of Health Care, Vilniaus kolegija/Higher Education Institution, Didlaukio str. 45, Vilnius LT–08303, Lithuania
[2]Institute of Biosciences, Vilnius University, Saulėtekio av. 7, Vilnius LT–10257, Lithuania
[3]Center for Physical Science and Technology, Saulėtekio av. 3, Vilnius LT–10257, Lithuania
[4]JSC "Kvapų namai", Popieriaus g. 15, Vilnius LT–08404, Lithuania
*Corresponding author, E-mail: r.bikmurzin@spf.viko.lt

Key words: antimicrobials, essential oils, skin pathogens.

The rise of multidrug-resistant pathogens poses a growing threat to public health, highlighting the need for alternative antimicrobial strategies. Essential oils (EOs) are natural substances with known antibacterial, antifungal, and antiviral properties.

This study investigates the antimicrobial effect of pure essential oils and EO blends against clinically relevant skin pathogens: *Staphylococcus aureus, Streptococcus pyogenes, Escherichia coli, Pseudomonas aeruginosa, Candida* spp. Pure essential oils used in this study were from *Melauleca alternifolia* (P1), *Eucalyptus globulus* (P2), *Pinus sylvestris* (P3), *Citrus limon* (P4), *Thymus hyemalis* (P5). Oil blends M1 – M5 are presented in Table 1.

Essential oil blends and pure oils were provided and their chemical composition was determined by JSC "Kvapų namai" using gas chromatography-mass spectrometry.

MICs were estimated by broth microdilution method in sterile 96-well microplates. Bacteria were subcultured on TSA and yeasts on Sabouraud agar 48 h prior testing. Homogeneous micellar aggregates of sterile distilled water and each essential oil at a 1:1 (*v*/*v*) ratio were produced by sonication at 40 kHz for 20 min, creating working stock solution. Stock working solution (200 µL) was added to the first well, and 100 µL of 2X broth (Mueller-Hinton for bacteria or YPD for yeasts) to wells 2 to 12, followed by two-fold serial dilutions to reach final concentration of 50 to 0.025% (*v*/*v*). Plates were incubated aerobically at 35 °C for 18 h and the MIC was considered the lowest essential oil concentration without visible growth. Minimum bactericidal concentrations (MBCs) were determined from the last five wells of each microplate row that showed no visible growth after MIC incubation using spot-inoculation on agar with 5 µL from each corresponding well. The MBC was defined as the lowest essential oil concentration (*v*/*v* of the stock solution) that resulted in no colony growth on the agar surface after overnight incubation at 35 °C under aerobic conditions (Man et al. 2019).

Among the tested samples, several EO blends exhibited synergistic antibacterial activity, resulting in reduced MIC values against multiple pathogens (Fig. 1). Best overall growth inhibition was achieved by pure essential oil P3 from *Pinus sylvestris* on all tested strains, except *Pseudomonas aeruginosa*. Great inhibitory activity was shown by EOs P1, P4, M2 and M4 with concentration mean of about 1%. The Kruskal-Wallis test did not show statistically significant differences in MIC values among the tested oils (χ^2 = 12.66, df = 9, p = 0.179), which was confirmed by post-hoc pairwise comparisons with Bonferroni adjustment (all adjusted $p > 0.05$).

MBC value (Fig. 2) distribution followed a similar pattern to MICs but with higher values overall. The Kruskal-Wallis test indicated no statistically significant differences

Table 1. Essential oil blend formulation by source

Code	Source
M1	*Picea mariana, Citrus limon, Thymus zygis, Eucalyptus globulus, Melauleca alternifolia*
M2	*Melauleca alternifolia, Pinus sylvestris, Cimbopogon martini* var. *motia, Eucalyptus globulus, Thymus hyemalis*
M3	*Melauleca alternifolia, Pinus sylvestris, Boswellia carterii, Ravensara aromatica, Rosmarinus officinalis, Cimbopogon citratus*
M4	*Eucalyptus globulus, Abies balsamea, Eucalyptus radiata, Cinnamonum camphora* var. *linaloolifera, Backhousia citriodora, Eucalyptus staigerania*
M5	*Cinnamomum camphora, Rosmarinus officinalis, Citrus limon, Eucalyptus globulus, Eugenia caryophylus, Cinnamonum cassia*

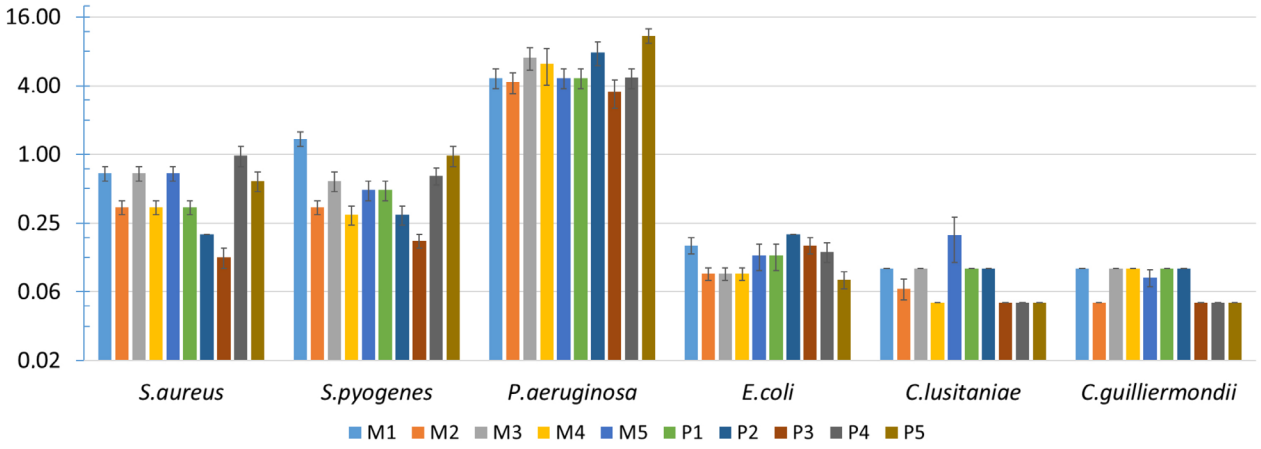

Fig. 1. MIC values (%) of pure essential oils (P1 – P5) and oil blends (M1 – M5) $\log_2$ scale. Average of 3 replicates ± standard deviation.

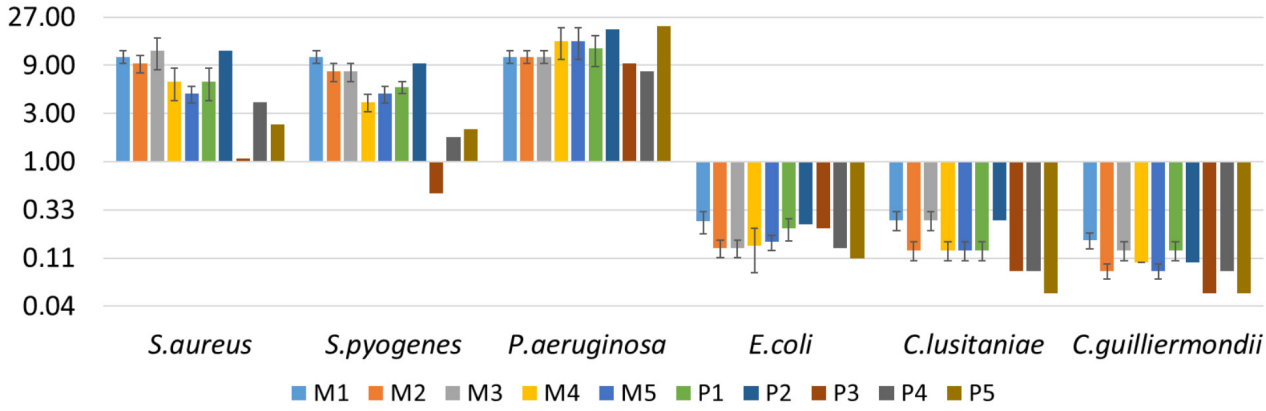

Fig. 2. MBC values (%) of pure essential oils (P1 – P5) and oil blends (M1 – M5) $\log_3$ scale. Average of 3 replicates ± standard deviation.

in bactericidal activity across oil formulations (χ^2 = 1.93, df = 9, p = 0.993). Pairwise post-hoc comparisons with Bonferroni adjustment confirmed that none of the oil pairs differed significantly (all adjusted $p > 0.05$).

Notably, *Pseudomonas aeruginosa* was the most resistant across the tested organisms, with MICs of 4.7% for blends and improved MBCs values of blends over pure oils (e.g. P2 vs M2 from 20.3 to 10.9%), indicating a possible synergistic effect. Mixtures containing *Melaleuca alternifolia* and *Pinus sylvestris* exhibited improved antimicrobial activity against several pathogens.

Despite this study did not find statistically significant improvement of EO blend antimicrobial activity, these results highlight the potential of EO blends and support formulation as a key factor in enhancing efficacy. Further research should explore the mechanisms of synergy and develop optimized blends formula.

Acknowledgements

Experiments conducted with financial support of Applied scientific research, experimental development and art activities of Vilniaus kolegija/Higher Education Institution and JSC "Kvapų namai". We thank Prof. Dr. Eglė Lastauskienė and Dr. Kotryna Čekuolytė from the Department of Microbiology and Biotechnology, Institute of Biosciences, Life Sciences Centre, Vilnius University, for the provided microorganisms.

References

Man A., Santacroce L., Jacob R., Mare A., Man L. 2019. Antimicrobial activity of six essential oils against a group of human pathogens: a comparative study. *Pathogens* 8: 15.

Mycelium biocomposites derived from agricultural and wood processing byproducts with magnetic properties as potential biosorbent

Oskars Bikovens[1]*, Mikhail Maiorov[2], Ilze Irbe[1]

[1]Latvian State Institute of Wood Chemistry, Riga LV–1006, Latvia
[2]Institute of Physics, University of Latvia, Miera 32, Salaspils LV–2169, Latvia
*Corresponding author, E-mail: oskars.bikovens@kki.lv

Key words: biosorbents, magnetic properties, mycelium biocomposites.

Adsorption of heavy metals on biosorbents is attractive approach to remediate the wastewater. Birch sanding dust (BSD) and wheat straw (WS) are studied as biosorbent and they are suitable for mycelium based bio-composites (MBBs) production. There is a growing interest in magnetic bio-sorbents (Ghotekar et al. 2022). Magnetic sorbent has the advantage of separating substances from the solution by a magnetic field without additional centrifugation or filtration. The present study aimed to develop the MBBs from BSD and WS, and modify them with magnetite (Fe_3O_4) micronanoparticles.

The lignocellulose substrates for the development of MBB were obtained from the local industry. Wheat straw was obtained from the Latgale Agricultural Science Center (Vilani, Latvia), and birch (*Betula pendula*) sanding dust from the plywood producer Latvijas Finieris. MBBs were produced from *Trametes versicolor* mycelium grown on BSD and WS by the method of Irbe et al. (2024).

Magnetic particles were synthesized by co-precipitation method. MBBs were suspended in water, added $FeCl_2$ and $FeCl_3$ and NH_3 water solution under argon atmosphere. The obtained magnetic MBBs particles were separated with a magnet, washed and dried. The obtained magnetic MBBs were investigated with a Leica DMLB light microscope. The images were captured with a Leica DFC490 video camera using calibrated image analysis software (Image-Pro plus 6.3, Media Cybernetics, Inc.). The magnetic properties of the obtained magnetic MBBs were analyzed using vibrating sample magnetometry with a Lake Shore Cryotronics instrument 7404VSM (OH, USA). The obtained magnetic bio-composites were magnetized within a region of uniform magnetic-flux density with variable strength (–10 to +10 kOe) and subjected to vibrational excitation at low frequency, and the magnetic moment of the sample was deduced (Maiorov et al. 2019).

The obtained magnetite micro/nanoparticles particles (particle size < 30 μm) and magnetic birch sanding dust mycelium bio-composites showed magnetization curves with no hysteresis typical for superparamagnetics (Fig. 1, 2). Saturation mass magnetization of obtained magnetite was as high as 65.2 emu g^{-1}. Saturation magnetization of the magnetic birch sanding dust mycelium composites was 7.8 emu g^{-1}.

Saturation magnetization (Ms) of magnetic bio-

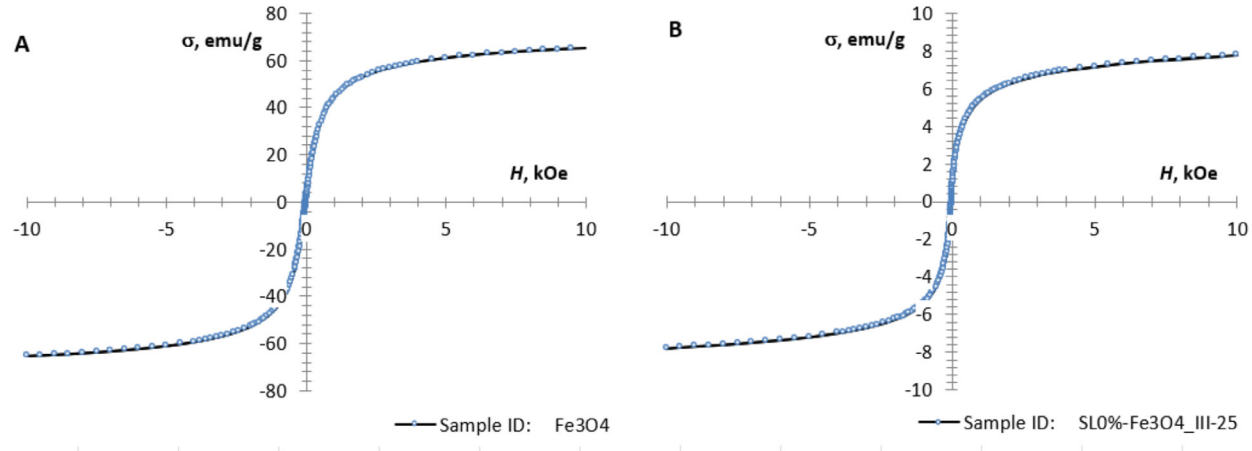

Fig. 1. Magnetization curve of obtained magnetite (A) and the magnetic birch sanding dust mycelium composites (B).

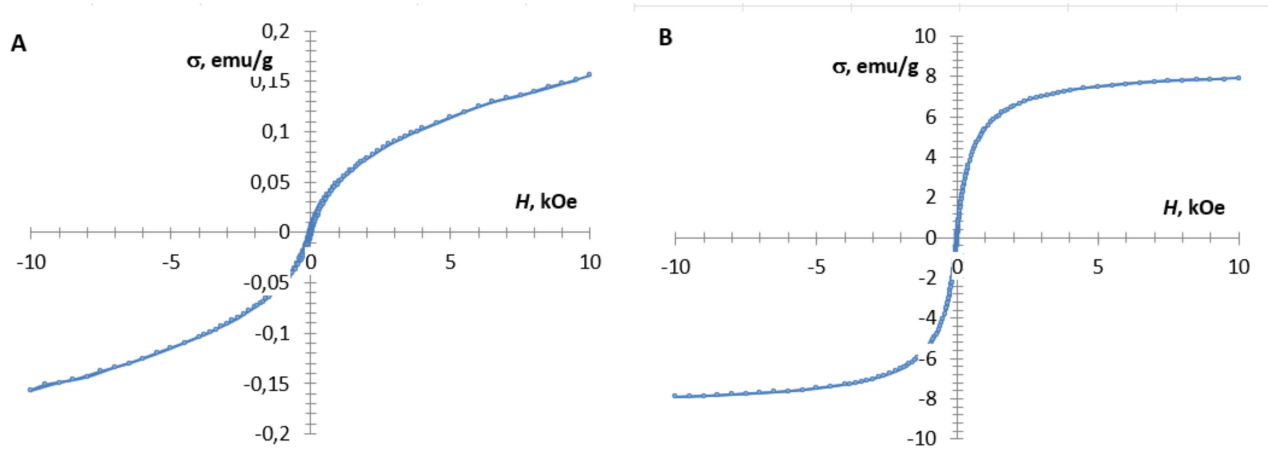

Fig. 2. Magnetization curve of the magnetic wheat straw mycelium bio-composites (A) and magnetic wheat straw composite (B).

composite with wheat straw was much lower 0.16 emu g^{-1}. Calculated magnetite concentration in the bio-composite was 0.2%. In comparing synthesis of magnetic bio composites with initial wheat straw showed Ms = 7.9 and calculated magnetite concentration 12% that is close to the magnetic birch sanding dust mycelium bio-composites. Probably wheat straw mycelium bio-composite inhibit synthesis of magnetite micro/nanoparticles.

In conclusion, obtained results showed that co-precipitation of magnetite with birch sanding dust mycelium based bio-composites is a perspective method for magnetic bio-sorbent synthesis on base of mycelium composite. Synthesis of magnetite micro/nanoparticles with wheat straw mycelium bio-composites was not so successful. Probably wheat straw mycelium bio-composite inhibit synthesis of magnetite.

Acknowledgements

This research was funded by the Latvian Research Council FLPP project No. lzp-2023/1-0633 "Innovative mycelium biocomposites (MB) from plant residual biomass with enhanced properties for sustainable solutions".

References

Ghotekar S., Murthy H.C.A., Roy A., Bilal M., Oza R. 2022. Magnetic nanomaterials-based biosorbents. In: Denizli A., Ali N., Bilal M., Khan A., Nguyen T.A. (Eds.) *Nano-Biosorbents for Decontamination of Water, Air, and Soil Pollution*. Elsevier, Amsterdam, pp. 605–614.

Irbe I., Kirpluks M., Kampuss M., Andze L., Milbreta U., Filipova I. 2024. Assessing the conformity of mycelium biocomposites for ecological insulation solutions. *Materials* 17: 6111.

Maiorov M.M., Zablotsky D., Blums E., Krumina A. 2019. Model colloids to study surface-ligand interactions in nanosized Fe_3O_4. *IOP Conf. Ser. Mater. Sci. Eng.* 503: 012029.

Misconceptions about nucleic acids signatures in FTIR spectroscopy

Mara Grube*, Karlis Shvirksts

Institute of Microbiology and Biotechnology, University of Latvia, Jelgavas 1, Riga LV–1004, Latvia
*Corresponding author, E-mail: mara.grube@lu.lv

Key words: DNA, FTIR spectroscopy, RNA.

Fourier transform infrared (FTIR) spectroscopy provides molecularly specific signatures of biological structure and function in a rapid and non-invasive manner. Consequently, it is widely used to detect structural and compositional changes in cells and tissues. Spectral interpretation relies on assigning absorption bands to individual biochemical components. However, a persistent misconception in the literature is the attribution of the band near 1080 cm^{-1} as a direct and unique marker of DNA and RNA content in biomass.

Biological samples are complex, multicomponent systems, and their FTIR spectra represent a superposition of signals from all constituent macromolecules. Moreover, these macromolecules share many common functional groups, which leads to extensive band overlap. Therefore, reliable interpretation requires the acquisition of reference spectra from pure component standards and their mixtures at varying concentrations, followed by appropriate spectral processing, development of quantitative analysis methods, and validation through comparison with known concentrations. This systematic workflow was applied in our previous studies on quantitative FTIR analysis of various biosamples (Grube et al. 1999; Grube et al. 2002). Representative spectra of the main macromolecular classes are shown in Fig. 1.

For carbohydrates, proteins, and lipids, the most intense absorption bands serve as practical marker bands: approximately 1080 cm^{-1} for carbohydrates; ~1660 and 1550 cm^{-1} (amide I and amide II) for proteins; and the regions 2800–3000 cm^{-1} and 1744 cm^{-1} for lipids. In nucleic acid spectra, the strongest absorption bands arise from PO_2^- stretching vibrations at ~1093 cm^{-1} and 1225 – 1241 cm^{-1}, C–O stretching vibrations in the 1050 – 1080 cm^{-1} region, and base vibrations between 1608 and 1697 cm^{-1}. Quantitative FTIR methods have therefore been developed using the most intense bands while explicitly accounting for spectral overlap. Characteristic spectral regions of main macromolecular classes in biomass are shown in Fig. 2.

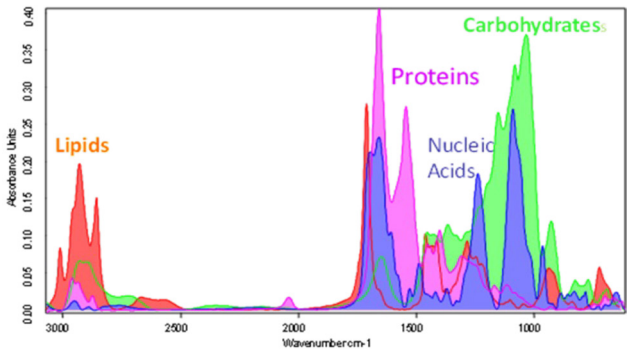

Fig. 1. FTIR spectra of carbohydrates (glycogen), proteins (BSA), lipids (cardiolipin), and nucleic acids (salmon testes DNA).

Results from multiple quantitative studies (Grube et al. 1999; Grube et al. 2002; Grube et al. 2018; Leonova et al. 2020; Jouhet et al. 2024) clearly demonstrate that the 1050 – 1080 cm^{-1} region cannot be considered a specific marker for nucleic acids. This region reflects PO_2^- stretching vibrations not only from nucleic acids but also from membrane phospholipids, and it further overlaps with C–O stretching vibrations from carbohydrates such as glycogen. In addition, nucleic acids constitute only a minor fraction of total cellular biomass, and their spectral contribution is therefore weak compared with those of proteins, lipids,

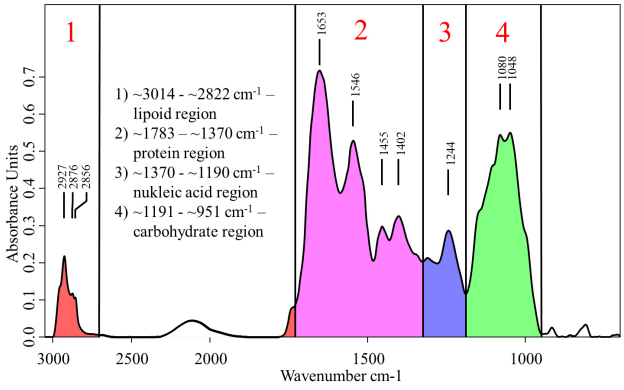

Fig. 2. Characteristic spectral regions used for identification of carbohydrates, nucleic acids, proteins, and lipids in biosamples (*Saccharomices cerevisiae* shown as an example), where (1) ~3014 – ~2822 cm^{-1} lipid region, (2) ~1783 – ~1370 cm^{-1} protein region, (3) ~1370 – ~1190 cm^{-1} nucleic acid region, (4) ~1191 – ~951 cm^{-1} carbohydrate region.

and carbohydrates, which dominate the FTIR fingerprint region.

Consequently, the most reliable marker band for nucleic acids in FTIR spectra is the PO_2^- asymmetric stretching vibration in the 1230 – 1250 cm^{-1} range. This clarification underscores that FTIR spectroscopy provides a holistic biochemical fingerprint rather than a DNA- or RNA-specific probe, and that careful band assignment is essential for meaningful biological interpretation. Misinterpretation of the 1080 cm^{-1} band may therefore lead to erroneous conclusions regarding nucleic acid concentration, integrity, or mutational status.

References

Grube M., Zagreba J., Gromozova E., Fomina M. 1999. Comparative investigation of the macromolecular composition of mycelia forms *Thielavia terrestris* by infrared spectroscopy. *Vibr. Spec.* 19: 301–306.

Grube M., Bekers M., Upite D., Kaminska E. 2002. IR-spectroscopic study of *Zymomonas mobilis* and levan precipitate. *Vibr. Spec.* 28: 277–285.

Grube M., Shvirksts K., Krafft Chr., Kokorevicha S., Zandberga E., Abols A., Line A., Kalnenieks U. 2018. Miniature diamond-anvil cells for FTIR-microspectroscopy of small quantities of biosamples. *Analyst* 143: 3595–3599.

Leonova E., Shvirksts K., Borisovs V., Smelovs E., Sokolovska J., Bisenieks E., Duburs G., Grube M., Sjakste N. 2020. Spectroscopic and electrochemical study of interactions between DNA and different salts of 1,4-dihydropyridine AV-153. *PeerJ* 8: e10061

Jouhet J., Alves E., Boutté Y., Darnet S., Domergue F., Durand T., Fischer P., Fouillen L., Grube M., Joubès J., Kalnenieks U., Kargul J.M., Khozin-Goldberg I., Leblanc C., Letsou S., Lupette J., Markovj G. V., Medina I., Melo T., Mojzeš P., Momchilova S., Mongrand S., Moreira A.S.P., Neves B.B., Oger C., Rey F., Santaeufemia S., Schaller H., Schleyer G., Tietel Z., Zammit G., Ziv C., Domingues R. 2024. Plant and algal lipidomes: analysis, composition, and their societal significance. *Progr. Lipid Res.* 96: 101290.

Fourier-transform infrared spectroscopy – a multifunctional tool in microbiological research

Karlis Shvirksts*, Mara Grube

Institute of Microbiology and Biotechnology, University of Latvia, Jelgavas 1, Riga LV–1004, Latvia
*Corresponding author, E-mail: karlis.svirksts@lu.lv

Key words: biofilms, chemometrics, diamond anvil cell, FTIR spectroscopy, high-throughput screening, infrared microscopy.

Microbiological research often requires methods that rapidly differentiate strains, track metabolic states, and detect structural adaptations such as biofilm formation or stress-induced biochemical remodelling. Conventional phenotypic assays and molecular approaches provide valuable information but can be labour-intensive, marker-dependent, or poorly suited to capturing the integrated biochemical state of cells. Fourier-transform infrared (FTIR) spectroscopy offers a complementary, label-free alternative by recording vibrational spectra that reflect the combined contributions of proteins, lipids, nucleic acids, and polysaccharides in intact microbial material (Naumann 2001; Winder et al. 2004). When performed under standardized cultivation and sampling conditions, FTIR yields highly reproducible "biochemical fingerprints" suitable for classification and physiological monitoring.

A major practical advantage of FTIR spectroscopy is its modularity: measurement configurations can be selected according to sample properties, biomass availability, and required spatial or throughput resolution. Classical transmission measurements using potassium bromide (KBr) pellets remain valuable when detailed characterization of dried biomass or extracted biomolecules is required. In this workflow, microbial material is dried, homogenized with IR-transparent KBr, and pressed into a pellet, yielding high-quality spectra with strong signal-to-noise characteristics. However, the method is time-consuming and moisture-sensitive, making it best suited for reference measurements or targeted structural comparisons rather than routine screening.

For comparative microbiology and phenotyping studies involving many strains or conditions, high-throughput screening extensions (HTS-XT) substantially improve scalability and standardization. HTS-XT workflows rely on depositing controlled amounts of biomass onto IR-transparent substrates in multi-well formats, followed by automated spectral acquisition. This platform supports rapid profiling of large strain collections, screening of mutant libraries, and monitoring of biochemical shifts associated with growth phase transitions or exposure to antimicrobial compounds (Winder, Godacre 2004). Reduced operator intervention improves reproducibility and supports generation of robust datasets suitable for multivariate modelling.

Infrared microscopy extends FTIR spectroscopy into the spatial domain and is particularly informative for structured microbial systems. Using conventional IR objectives or attenuated total reflection (ATR) optics, FTIR microscopy enables micrometre-scale mapping of biochemical heterogeneity within complex samples. This is especially relevant for biofilms and microbial consortia, where gradients in nutrients, metabolites, and local stressors drive spatially distinct physiological states (Schmitt, Flemming 1998). ATR-based measurements are well suited to surface-associated phenomena, including microbial adhesion and extracellular polymeric substance production, as they preferentially probe material in close contact with the ATR crystal.

When sample quantity is limited – such as in rare isolates, slow-growing organisms, microcultures, or valuable environmental specimens – diamond anvil cell (DAC) technology enables acquisition of high-quality FTIR spectra from minimal biomass. By confining small sample volumes between diamond anvils while maintaining optical access, DAC measurements allow reliable spectral acquisition with substantially reduced material requirements. This extends FTIR applicability to microbiological questions where conventional sampling would otherwise be prohibitive, as demonstrated using DAC-assisted FTIR microspectroscopy for analysis of very small quantities of biosamples (Grube et al. 2018).

Across these measurement modes, the interpretive power of FTIR spectroscopy depends strongly on chemometric and statistical analysis. Because microbial FTIR spectra integrate signals from many overlapping biochemical bands, multivariate approaches are required to resolve biologically meaningful variation. Unsupervised methods, such as principal component analysis and hierarchical clustering, support exploratory profiling, identification of dominant spectral variance, and detection of outliers.

Supervised approaches – including discriminant analysis and machine-learning classifiers – enable reproducible discrimination at the genus, species, and, under suitable conditions, strain level, particularly when combined with curated reference libraries and rigorous quality control of cultivation and measurement protocols.

Taken together, the FTIR toolkit provides a flexible analytical framework that bridges classical microbiological phenotyping with rapid biochemical profiling. By selecting appropriate measurement modules (KBr transmission, HTS-XT, microscopy/ATR, or DAC) and combining them with robust chemometric workflows, FTIR spectroscopy supports microbial identification, monitoring of metabolic dynamics, and characterization of structural and stress-related adaptations. Continued development of interoperable spectral libraries, harmonized protocols, and transparent modelling pipelines will further enhance the transferability of FTIR-based phenotyping across laboratories and application domains (Naumann 2001; Lasch 2012).

References

Grube M., Shvirksts K., Krafft C., Kokorevicha S., Zandberga E., Abols A., Line A., Kalnenieks U. 2018. Miniature diamond-anvil cells for FTIR-microspectroscopy of small quantities of biosamples. *Analyst* 143: 3595–3599.

Lasch P. 2012. Spectral pre-processing for biomedical vibrational spectroscopy and microspectroscopic imaging. *Chemometr. Intell. Lab. Syst.* 117: 100–114.

Naumann D. 2001. FT-infrared and FT-Raman spectroscopy in biomedical research. *Appl. Spectrosc. Rev.* 36: 239–298.

Schmitt J., Flemming H.-C. 1998. FTIR-spectroscopy in microbial and material analysis. *Int. Biodeterior. Biodegrad.* 41: 1–11.

Winder C.L., Godacre R. 2004. Comparison of diffuse-reflectance absorbance and attenuated total reflectance FT-IR for the discrimination of bacteria. *Analyst* 129: 1118–1122.

First look at antibiotic consumption and resistance genes in urban wastewater in Latvia

E. Bebre[1]*, A. Cīrulis[2,3], J. Ķibilds[1]

[1]Institute of Food Safety, Animal Health, and Environment "BIOR", Lejupes 3, Riga LV–1076, Latvia
[2]Faculty of Medicine and Life Sciences, University of Latvia, Jelgavas 1, Riga LV–1004, Latvia
[3]Latvian Biomedical Research and Study Centre, Ratsupites 1 k-1, Riga LV–1067, Latvia
*Corresponding author, E-mail: evija.bebre@bior.lv

Key words: antibiotic consumption antibiotic resistance, digital PCR, monitoring urban wastewater.

The mortality rate associated with antimicrobial resistance (AMR) in people older than five has increased significantly between 1990 and 2021. Thus, AMR is a crucial burden on public health. It is critical to monitor the spread of resistance and investigate the factors driving it (GBD 2021 Antimicrobial Resistance Collaborators 2024). Wastewater monitoring has emerged as an effective approach to detect pathogens and AMR at the population level (Sun et al. 2022). This study aimed to investigate the impact of antibiotic consumption on the abundance of antibiotic resistance genes (ARGs) in urban wastewater.

Influent samples were collected from seven urban wastewater treatment plants in Latvia – Rīga, Liepāja, Ventspils, Jelgava, Rēzekne, Daugavpils, and Valmiera. Sampling was done from autumn 2022 to winter 2024. The concentration of selected ARGs – *sul1*, *tetW*, and *ermB*, and 16S rDNA – was determined in the samples using digital PCR. Antibiotic consumption data were acquired from Latvia's Centre for Disease Prevention and Control. Data analysis was performed in R (4.5.1), using linear regression models for correlation between antibiotic consumption and ARG numbers. ANOVA was used to determine antibiotic consumption and seasonal differences.

It was determined that *sul1* and *tetW* abundance was seasonal but *ermB* had a tendency to decrease during the study period (Fig. 1). Based on antibiotic consumption, it was determined that season had a statistically significant effect on doxycycline ($F = 6.66$; $p = 0.0245$) (Fig. 2) and azithromycin consumption ($F = 6.22$; $p = 0.0285$) (Fig. 3).

Additionally, doxycycline consumption statistically significantly affected *tetW*/16S rDNA abundance in wastewater with a three-month lag period ($F = 6.63$; R^2

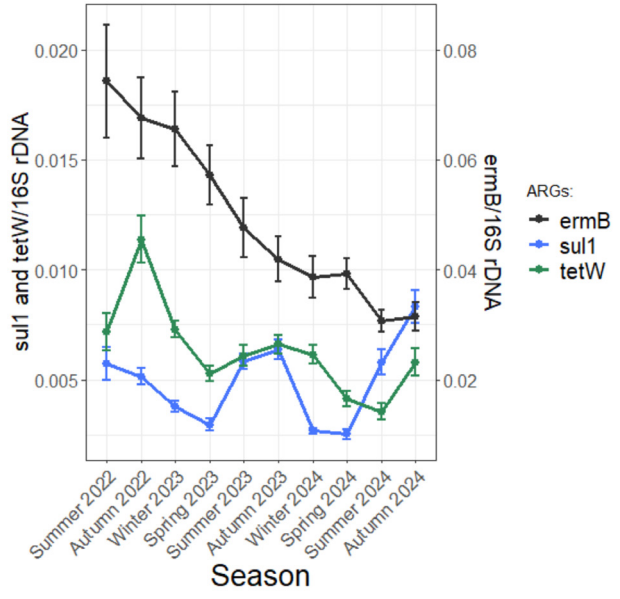

Fig. 1. ARGs – *sul1, tetW*, and *ermB* – abundance during the study period with standard error ($n = 3$). ARGs quantity normalised with 16S rDNA.

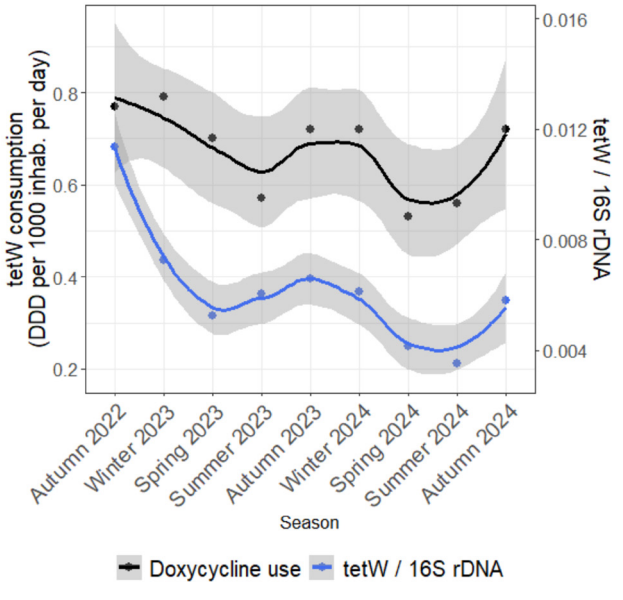

Fig. 2. Doxycycline consumption in Latvia and average *tetW*/16S rDNA abundance during the study period. Doxycycline consumption is shown with a three-month lag period.

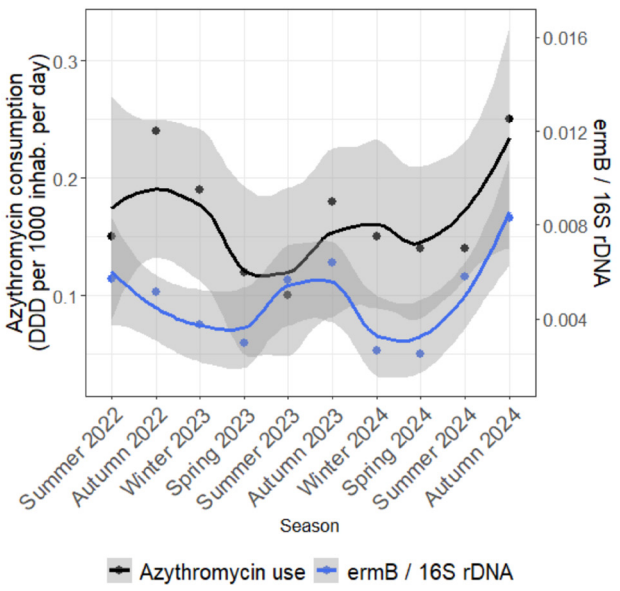

Fig. 3. Azithromycin consumption and *ermB*/16S rDNA abundance in Latvia during the study period.

= 0.41; p = 0.0367). No significant effect of doxycycline consumption and *tetW*/16S rDNA abundance with neither no lag period nor a six-month lag period was found.

No statistically significant effect was found between *sul1*/16S rDNA and sulfamethoxazole and trimethoprim, as well as between *ermB* and clarithromycin, azithromycin, and clindamycin consumption ($p > 0.05$). Additionally, no statistically significant effect ($p > 0.05$) was found between antibiotic consumption and the year, implying no significant difference in antibiotic consumption between years 2022 and 2024.

Observed results show complicated relationships between antibiotic resistance, antibiotic consumption, and the urban environment. These findings reveal the differences in interactions between antibiotic consumption, season and their respective ARGs, suggesting that a tailored approach is necessary for each monitored ARG.

Acknowledgements

Research was funded by the project VPP-EM-BIOMEDICĪNA -2022/1-0001.

References

GBD 2021 Antimicrobial Resistance Collaborators. 2024. Global burden of bacterial antimicrobial resistance 1990-2021: a systematic analysis with forecasts to 2050. *Lancet* 404: 1199–1226.

Sun D.S., Kissler S.M., Kanjilal S., Olesen S.W., Lipsitch M., Grad Y.H. 2022. Analysis of multiple bacterial species and antibiotic classes reveals large variation in the association between seasonal antibiotic use and resistance. *PLoS Biol.* 20: e3001579.

Comparative analysis of microbial growth dynamics using laser speckle imaging and conventional liquid culture methods

E. T. Mincis[1]*, V. Liepiņš[1], I. Ļihačova[1], A. Ļihačovs[1], J. Liepiņš[2]

1Institute of Atomic Physics and Spectroscopy, University of Latvia, Jelgavas 1, Riga LV–1004, Latvia
2Institute of Microbiology and Biotechnology, University of Latvia, Jelgavas 3, Riga LV–1004, Latvia
*Corresponding author, E-mail: mincis.teodors@gmail.com

Key words: antimicrobial susceptibility, laser speckle imaging, real-time monitoring, *Saccharomyces cerevisiae*.

Microbial growth assessment is critical for applications ranging from antimicrobial susceptibility testing to industrial bioprocess optimization. While conventional methods like optical density (OD_{600}) measurements in 96-well plates are standard, they often lack the temporal resolution to capture rapid physiological changes. Laser speckle imaging (LSI), combined with subpixel correlation analysis, has demonstrated potential for early detection of antibacterial susceptibility by visualizing dynamic changes in microbial activity (Balmages et al. 2021; Balmages et al. 2023). This study aims to compare the efficacy of LSI with conventional liquid culture methods for real-time monitoring of microbial growth under varying inhibitory conditions.

This study focuses on testing the ability of LSI system to detect the growth pattern of *Saccharomyces cerevisiae* CEN. PK. Comparison of LSI and conventional culture growth monitoring in 96-well plates by OD measurements are being done under standard conditions and in the presence of inhibitors, such as antimicrobial agents or environmental stressors. LSI is capturing spatiotemporal activity patterns of the colony growth, while OD_{600} measurements serve as a benchmark. The correlation between activity signals acquired by LSI and OD_{600} data is analysed to assess the sensitivity, speed, and accuracy of LSI in detecting growth inhibition.

Laser Speckle Imaging Setup A 660 nm, 120 mW laser diode (HL6545MG, Thorlabs) with an aspheric collimating lens (LD2297-A) provided uniform illumination. Backscattered light from *Saccharomyces cerevisiae* (CEN. PK 113-7A) macrocolonies – grown on YPD agar with 1% activated charcoal – was polarized and focused onto an event-based sensor (Metavision IMX636, 1280 × 720 pixels) via an 8 mm C-mount lens (f/9.5). The sensor captured speckle patterns asynchronously (3000 to 5000 effective fps), resolving speckle grains (6.3 μm). Colonies were treated with 20 μL of 100 mM or 1 M metal ion solutions [$(NH_4)_2Cr_2O_7$, $CuSO_4$, $NiCl_2$] or distilled water (control), then imaged after 3 h of drying.

Growth Analysis Liquid cultures in 96-well plates (YPD medium) were monitored using a TECAN Infinite 200 Pro plate reader. At OD_{615} 0.4 to 0.6, metal ion solutions were added, and absorbance (615 nm) was recorded every 9.45 min over 47 h.

Data Processing Speckle activity maps (Fig. 1) were generated from event data, converted to 8-bit images in ImageJ, and thresholded to black/white. Microbial activity was calculated as the ratio of black to white pixels in each colony's region of interest. Activity was normalized to water-treated controls. OD data were background-corrected, and maximum OD values were normalized to controls. Normalized results from both laser speckle imaging (LSI) and OD measurements were compared (Fig. 2).

Microbial activity was assessed in the presence of $(NH_4)_2Cr_2O_7$, $CuSO_4$, and $NiCl_2$ at 100 mM and 1 M concentrations, with distilled water as the control.

For $(NH_4)_2Cr_2O_7$, LSI detected stronger inhibition than OD_{615}, especially at 1 M, where LSI showed near-complete inhibition (5.45% activity) compared to OD_{615} (14.19%

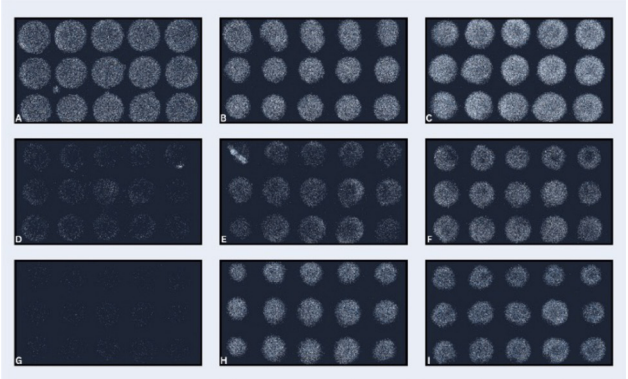

Fig. 1. Yeast macrocolony laser speckle patterns 3 h after treatment. A & B, no treatment; C, H_2O; D, 1 M $(NH_4)_2Cr_2O_7$; E, 100 mM $(NH_4)_2Cr_2O_7$; F, 100 mM $CuSO_4$; G, 1M $CuSO_4$; H, 100 mM $NiCl_2$; I, 1 M $NiCl_2$.

activity). $CuSO_4$ at 1 M also showed pronounced inhibition in LSI (1.45% activity) versus OD_{615} (15.42% activity). For $NiCl_2$, LSI and OD_{615} results were closer, but LSI still indicated slightly higher activity at 1 M (47.04 vs. 16.62%).

LSI demonstrated higher sensitivity to inhibitory effects, capturing rapid physiological changes due to its high temporal resolution. OD_{615} provided a more gradual detection of inhibition, reflecting cumulative biomass changes over time.

The correlation between LSI and OD_{615} was strongest at lower inhibitor concentrations but diverged at higher concentrations, where LSI detected more pronounced inhibition.

LSI's system has high temporal resolution which enables to capture rapid physiological changes, which may not be reflected in OD_{615} measurements taken at longer intervals. Therefore it's sensitivity could allow to detect growth inhibition more early than liquid culture. Indeed, for some metals we do observe fast and almost immediate lowering of signal in LSI system, like $(NH_4)_2Cr_2O_7$ or $CuSO_4$, however for $NiCl_2$ we observed the opposite – the signal decrease was not so sharp in comparison with OD measurements.

We think, that differences between Laser Speckle Imaging (LSI) and optical density (OD_{615}) measurements can be attributed to toxicity buffering effect of charcoal. The charcoal addition gave opportunity to lower background speckle effects from the reflections from media. However, this material also adsorbs metal ions and therefore lowers toxicity effects. In the same time liquid culture have homogeneous toxic compound distribution therefore intensifying the inhibitory effects of metal ions.

Yeast macrocolony structure and the distance to the neighbouring colony are the factors that can affect the colony resilience to heavy metals (Gaizer et al. 2024). In our current experiments, the distance to neighbouring macrocolonies where no more than 5 mm and initial cell number per macrocolony was high. When applying a droplet on those colonies, a diffusion of the compound occurs and the cells receive smaller the dose of the compound received by colony is less than that of the cells within the wells of 96 well plate. This effect must be taken into account to improve future experiments and developing of the system.

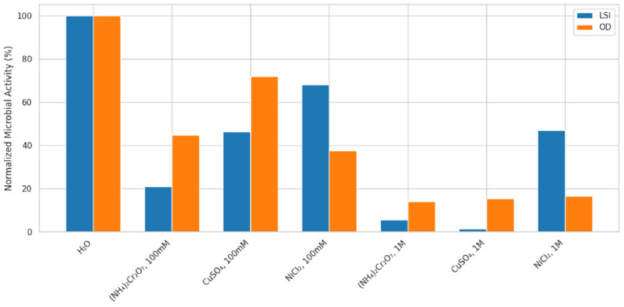

Fig. 1. Comparison of normalized microbial activity monitored with OD_{615} measurements in 96-well plate assays (orange bars) and LSI system (blue bars).

In summary, LSI and OD_{615} provide complementary insights into microbial growth dynamics. LSI offers enhanced sensitivity for detecting early physiological changes, while OD_{615} remains a robust method for quantifying biomass accumulation. Combining both methods could provide a more comprehensive understanding of microbial growth under inhibitory conditions.

Acknowledgements

The research was financed by the Recovery and Resilience Facility project "Internal and External Consolidation of the University of Latvia" (No.5.2.1.1.i.0/2/24/I/CFLA/007), grant project "High throughput laser speckle imaging to speed up experiments in microbiology", No. LU-BA-PA-2024/1-0072.

References

Balmages I., Liepins J., Zolins S., Bliznuks D., Lihacova I., Lihachev A. 2021. Laser speckle imaging for early detection of microbial colony forming units. *Biomed. Optics Expr.* 12: 1609–1620.

Balmages I., Reinis A., Kistkins S., Bliznuks D., Plorina E.V., Lihachev A., Lihacova I. 2023. Laser speckle imaging for visualization of hidden effects for early detection of antibacterial susceptibility in disc diffusion tests. *Front. Microbiol.* 14: 1221134.

Gaizer T., Juhász J., Pillér B., Szakadáti H., Pongor C.I., Csikász-Nagy A. 2024. Integrative analysis of yeast colony growth. *Commun. Biol.* 7: 511.